molecules

MDPI

Article

Assessing the Antinociceptive Potential of Flavonoids Isolated from *Boldoa purpurascens*: In Silico and In Vivo Approaches

Dulce M. González-Mosquera [1,2], Arelys López-Sacerio [1], Isabel Fraile-Gutiérrez [2], Roberto Díaz-Amador [3], Shaghayegh Jahangir [2], Emmy Tuenter [4], Anayancy Osorio-Madrazo [2,*] and Yudith Cañizares-Carmenate [3,*]

[1] Department of Pharmacy, Faculty of Chemistry and Pharmacy, Central University "Marta Abreu" of Las Villas, 54830 Santa Clara, Villa Clara, Cuba; dgonzalezmosquera@gmail.com (D.M.G.-M.); arelysls@uclv.edu.cu (A.L.-S.)
[2] Laboratory of Organ Printing, University of Bayreuth, 95447 Bayreuth, Germany; isabel.fraile.gutierrez@gmail.com (I.F.-G.); shaghayegh.jahangir@uni-bayreuth.de (S.J.)
[3] Laboratorio de Bioinformática y Química Computacional, Departamento de Medicina Traslacional, Facultad de Medicina, Universidad Católica del Maule, 3460000 Talca, Chile; rodiaz@ucm.cl
[4] Natural Products & Food Research and Analysis–Pharmaceutical Technology (NatuRAPT), Department of Pharmaceutical Sciences, University of Antwerp, 2610 Antwerp, Belgium; emmy.tuenter@uantwerpen.be
* Correspondence: ycanizares@ucm.cl (Y.C.-C.); anayancy.osorio-madrazo@uni-bayreuth.de (A.O.-M.)

Abstract

Analgesic therapy is crucial today due to its impact on the quality of life of patients suffering from diverse health conditions. Consequently, the search for new, natural therapeutic alternatives with few side effects remains a challenge for scientists. The main objective of this work was to identify new analgesic molecules by combining in silico strategies with in vivo experimental corroboration. In this regard, a robust, stable, and predictive QSAR-MLR model was developed that correlates the chemical structure of μ-receptor antagonist drugs with their biological activity. This model was used to predict the μ-opioid receptor-binding affinity of four natural flavonoids isolated from the species *Boldoa purpurascens*, and they were found to show good in silico activity profiles. Furthermore, these compounds were experimentally evaluated using the in vivo hot plate test in mice at doses of 50, 100 and 150 mg/kg. Among the evaluated flavonoids, 4′,5-dihydroxy-6,7-methylenedioxyflavonol-3-*O*-α-L-rhamnopyranosyl-(1→2)-β-D-glucopyranoside (DMR3) showed the most consistent antinociceptive response, particularly at doses of 100 and 150 mg/kg. However, its effects did not consistently exceed those of morphine, which was administered intraperitoneally, whereas the flavonoids were administered orally. Therefore, the comparison with morphine should be interpreted cautiously, considering the differences in dose and route of administration. The observed in vivo effects do not establish a specific μ-opioid receptor-mediated mechanism.

Keywords: *Boldoa purpurascens*; Nyctaginaceae; analgesic effect; hot plate test; multiple linear regression model; QSAR

Received: 2 November 2026
Revised: 21 November 2026
Accepted: 25 November 2026
Published: 27 November 2026

Copyright: © 2026 by the authors. Licensee MDPI, Basel, Switzerland. This article is an open access article distributed under the terms and conditions of the Creative Commons Attribution (CC BY) license.

1. Introduction

Pain is defined as an unpleasant sensory and emotional experience associated with actual or potential tissue damage [1]. It should be approached in a comprehensive manner, considering psychological, environmental, and somatic factors. Various types of pain

exist, among which acute pain and chronic pain stand out. Chronic pain affects the physical and psychological health of those who experience it, with repercussions on daily activities, autonomy, employment, and economic well-being. The impact of chronic pain of degenerative or inflammatory origin on quality of life is evident due to the limitations and consequences in physical, psychological, and social aspects [2,3].

Analgesics can act either peripherally or centrally, by modulating or inhibiting the synthesis of inflammatory and/or pain-mediating substances. Among the most commonly used analgesics are opioids and non-steroidal anti-inflammatory drugs [4]. Opioids, including morphine and its analogs, are the treatment of choice for severe pain. They interact with several closely related receptors known as opioid receptors, which are also affected by certain endogenous peptides such as enkephalins, endorphins, and dynorphins [5]. However, their use is associated with adverse effects, including tolerance, dependence, respiratory depression, vomiting, and constipation, among others [6]. The search for biocompatible natural products [7] for therapeutic alternatives remains a challenge.

Boldoa purpurascens Cav. (synonym *Salpianthus purpurascens* (Cav. ex Lag.) Hook. & Arn is a lesser-known wild plant species within the Nyctaginaceae family. In Cuba and other regions of the Americas, it grows in gardens and it is used in several countries as a diuretic and to treat urinary tract ailments [8]. Flavonoids are the secondary metabolites predominantly found in this plant and are known for their diverse pharmacological actions, including antioxidant [9,10], antihypertensive [11], diuretic [12], and anti-inflammatory [13] effects. However, there is a need to deepen the chemical and pharmacological study of this plant species.

As part of the experimental validation, in vivo experiments are performed [14,15]. However, the ethical limitations of using experimental animals are well known [16], which is why the use of computational strategies such as design, screening, or in silico evaluation methods is becoming increasingly common. These strategies aim not only to reduce the use of animals but also to lower costs and experimental time [17,18].

This study proposes an in silico evaluation of the μ-opioid receptor-binding affinity of four flavonoids isolated from *Boldoa purpurascens* [19], followed by experimental evaluation of their antinociceptive effects using the hot plate method.

2. Results

2.1. Cluster Analysis

In this work, a hierarchical agglomerative clustering method was applied to identify substructures in the standardized dataset, as well as repeated clusters or outliers. Given the total set of observations, the hierarchical strategy constructs a sequence of mergers that transforms the initial unitary clusters into a single final cluster. The dendrogram in Figure 1 represents the hierarchical output of the method, using Euclidean distance as a measure of comparison between cases and Ward's method as an indicator of cluster membership, selecting the merger that produces the lowest inter-cluster variance.

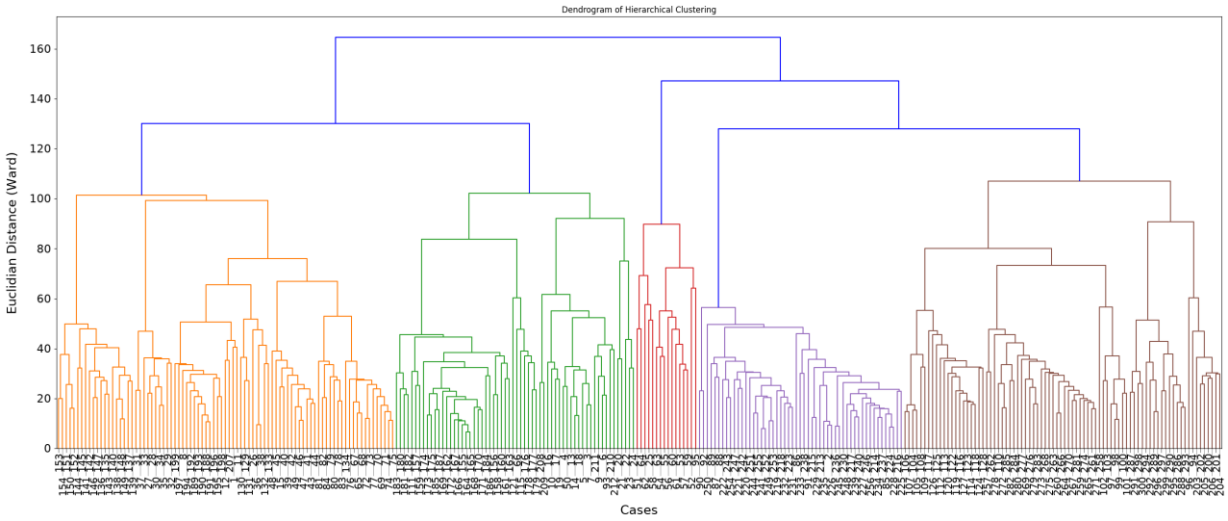


Figure 1. Dendrogram obtained from cluster analysis. Clusters 1–5 are distinguished by different colors.

No duplicates or outliers were detected in the study. Furthermore, five clusters were established from the dendrogram, each represented by a different color. This study served to divide the data into two series, randomly selecting 25% of each cluster for prediction and the remaining 75% for model training. The strategy used allowed for the structural representation of the different compound scaffolds in both series.

2.2. Modeling by Multiple Linear Regression

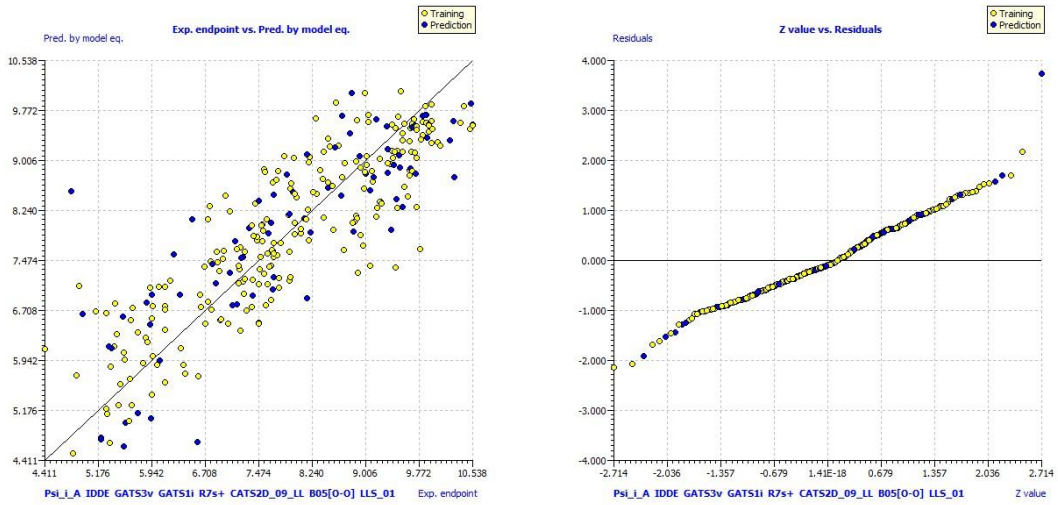
The resulting MLR model is shown in Equation (1) with its statistical parameters. The definition of the selected molecular descriptors can be seen in Table S2 of the Supporting Information.

$$\begin{aligned} pKi = 29.6 - 2.34x\mathbf{Psi_i_A} - 0.73x\mathbf{IDDE} - 5.41x\mathbf{GATS3v} - 4.66x\mathbf{GATS1i} \\ - 4.72x\mathbf{R7s+} - 0.08x\mathbf{CATS2D_09_LL} + 1.23x\mathbf{B05[O\text{-}O]} - 2.54x\mathbf{LLS_01} \end{aligned} \quad (1)$$

N = 225	R^2 = 0.7587	R^2_{adj} = 0.7498	$R^2 - R^2_{adj}$ = 0.0089
LOF = 0.5902	Kxx = 0.3093	Delta K = 0.0433	$RMSE_{TS}$ = 0.7136
MAE_{TS} = 0.5694	RSS_{TS} = 114.5725	CCC_{TS} = 0.8628	s = 0.7283
F = 84.9101			

Where N is the number of compounds in the training set, R^2 is the coefficient of determination, R^2_{adj} is the adjusted coefficient of determination, LOF is the Friedman lack-of-fit criterion, Kxx is the overall correlation between the descriptors, Delta K is the difference between the correlation between the descriptors (Kxx) and the correlation between the descriptors and the response (Kxy), $RMSE_{TS}$ is the root mean square error on the training calculation, MAE_{TS} is the mean absolute error in the fit calculated on the training set, RSS_{TS} is the sum of the squared residuals in the fit, s is the standard error of the estimate, CCC_{TS} is the correlation coefficient of agreement in training, and F is the Fisher F-value.

The experimental μ-opioid receptor binding constants (pKi) and the values predicted by the MLR model for the training set appear in Table S3 of the Supporting Information. Figure 2 shows the scatter plot of the predicted response versus the experimental response (a) and z-value versus residuals (b), which allow for easy detection of systematic trends or grouping of the data and, in addition, potential outliers in the data.

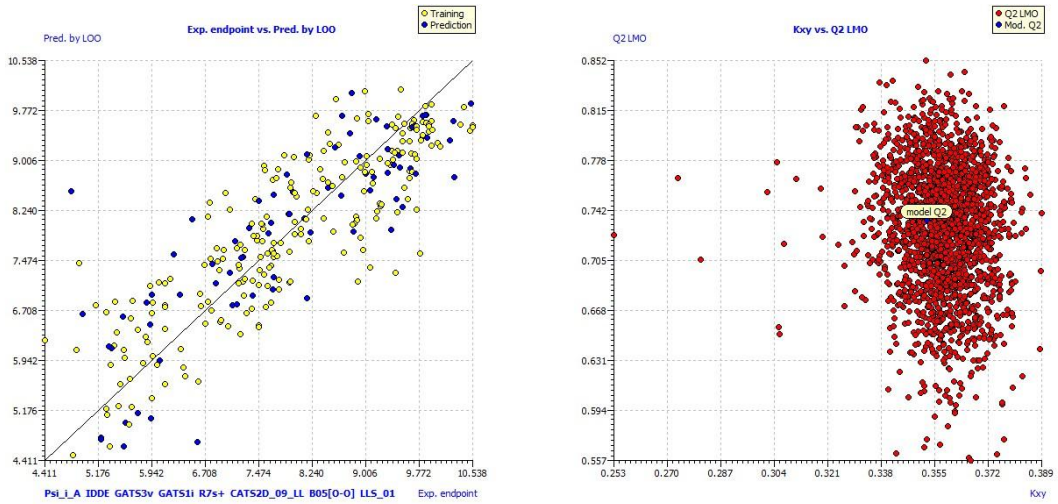


(**a**) (**b**)

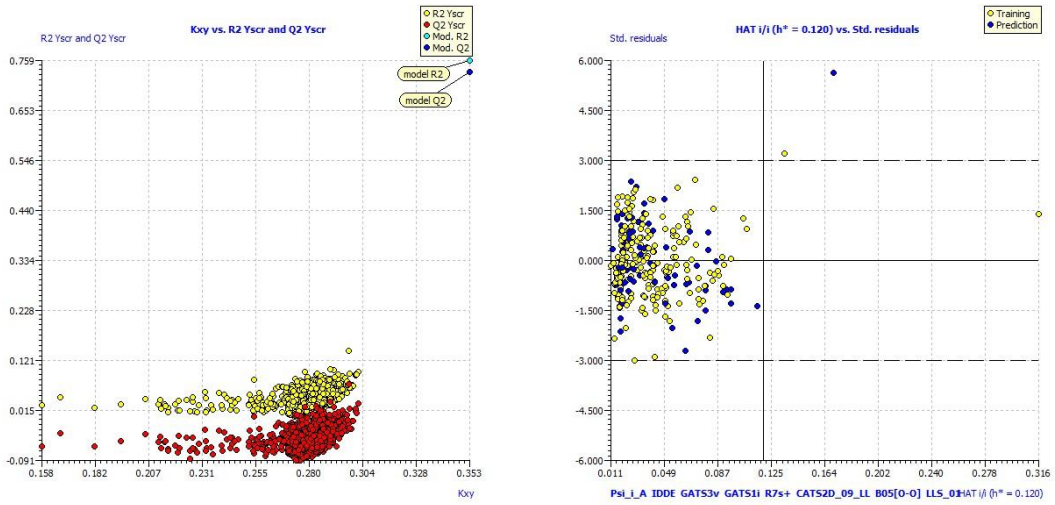
Figure 2. Model fit. The solid line represents the x = y reference line. (**a**) Scatter plot of the predicted versus the experimental response. (**b**) z-value versus residuals.

2.2.1. Validation

In the internal validation, Q^2_{LOO} and Q^2_{LMO} values of 0.7346 and 0.7316 were obtained, respectively, as well as R^2_{Yscr} values of 0.0356 and Q^2_{Yscr} of −0.0474 in the y-scrambling test. Figure 3 shows the results of the cross-validation: (a) observed vs. predicted values in the leave-one-out validation, (b) observations of each iteration of the leave-many-out validation, and (c) model performance in the y-scrambling test.



(**a**) (**b**)



(**c**) (**d**)

Figure 3. Model validation results. The solid line represents the x = y reference line. (**a**) Predictions by LOO. (**b**) Predictions in each LMO iteration. (**c**) y-scrambling test. (**d**) Applicability domain.

In the external validation (blue dots in Figure 2), the model yielded R^2_{PS} = 0.6895, $RMSE_{PS}$ = 0.8743, MAE_{PS} = 0.6816, $PRESS_{PS}$ = 57.3348, and CCC_{PS} = 0.8258. The Q^2-F1, Q^2-F2 and Q^2-F3 values were 0.6842, 0.6838 and 0.6378, respectively. Roy's statistics yielded average r^2m and Δr^2m values of 0.5708 and 0.1443. Additionally, the regression slopes obtained according to the Golbraikh and Tropsha criteria were k = 0.9935 and k′ = 0.9947, while the difference between R^2_0 and R'^2_0 was 0.0720. The relative deviation $|R'^2_0 - R'^2|/R'^2$ was 0.1111. The experimental and predicted values for the external set are shown in Table S4 of the Supporting Information.

In this study, the leverage (h) and standardized residuals approach described in the literature [20] was used to determine the chemical space where the model predictions are reliable. Figure 3d shows the William plot of the model for the training and prediction series.

2.2.2. Virtual Screening

Table 1 shows the pKi values predicted by the QSAR-MLR model for the compounds DMR 1–4 and their aglycone, as well as the category in which they are located according to the in silico study. Furthermore, Figure 4 shows the applicability domain plot of insubria for molecules that lack an experimental response, where the studied flavonoids are represented by red circles.

Table 1. pKi values predicted by the QSAR-MLR model in the virtual screening.

Name	Pred. by Model Equation	HAT i/i (h* = 0.1200)	Categories
DMR 1	7.6720	0.0901	Potent
DMR 2	9.2081	0.1038	Highly potent
DMR 3	7.7683	0.1136	Potent
DMR 4	6.1632	0.1793	Moderately potent
Aglycone	7.0920	0.2218	Potent

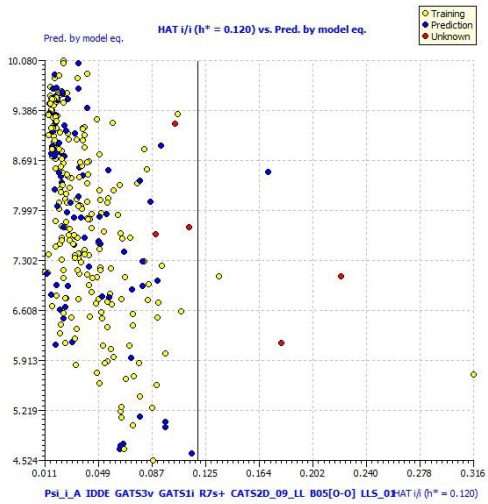


Figure 4. Insubria applicability domain of compounds.

2.3. Hot Plate Test

The recording of behavioral responses to pain and the determination of the percentage of analgesia by group, stratified by dose and time elapsed since administration can be seen in Table S6a–e of the Supporting Information. Table 2 shows the average reaction times for the natural compounds (DMR 1–4) at three dose levels, with the reference drug (morphine) and vehicle, at intervals of 30, 60, 90, and 120 min in the hot plate test. Figure 5 shows the percentages of antinociception achieved by the DMR 1–4 compounds compared to morphine and vehicle. Figure 6 represents the percentage of antinociception from flavonoids DMR 1–4 as the dose increases.

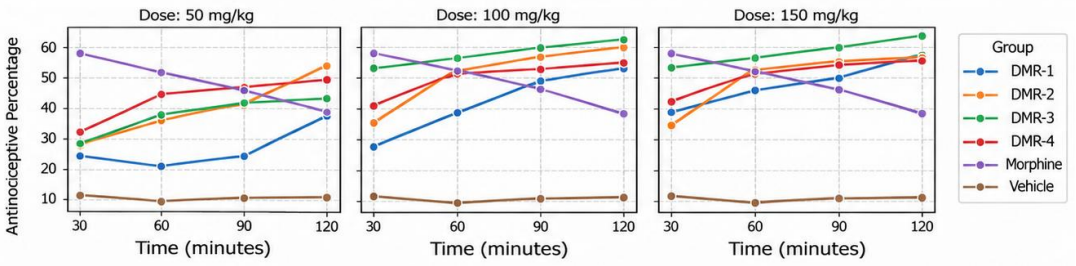


Figure 5. Percentages of antinociception in the hot plate test.

Table 2. Reaction time in the hot plate tests for the compounds of natural origin, morphine and vehicle.

Group	Dose (mg/kg)	Tb (s) ± S.D	Ta (s) ± S.D			
		0 min	30 min	60 min	90 min	120 min
Vehicle	100	8.00 ± 0.55	9.06 ± 0.20	8.88 ± 0.26	8.98 ± 0.37	9.00 ± 0.25
Morphine	7.5	7.84 ± 0.24	18.66 ± 0.45	16.38 ± 0.40	14.56 ± 0.41	12.78 ± 0.21
	50	7.02 ± 2.98	9.56 ± 4.20	9.04 ± 3.83	9.38 ± 3.89	11.46 ± 4.94
DMR 1	100	5.78 ± 2.91	8.02 ± 3.12	9.48 ± 3.88	11.38 ± 4.75	12.42 ± 5.30
	150	5.58 ± 2.48	9.72 ± 4.13	10.94 ± 4.59	11.70 ± 4.82	14.00 ± 5.83
	50	6.76 ± 2.94	9.42 ± 3.97	10.60 ± 4.37	11.44 ± 4.70	14.38 ± 5.88
DMR 2	100	6.21 ± 2.55	9.68 ± 4.02	12.98 ± 5.34	14.10 ± 5.77	15.26 ± 6.27
	150	6.40 ± 2.70	9.84 ± 4.15	13.48 ± 5.56	14.28 ± 5.84	14.76 ± 6.03
	50	7.65 ± 3.35	11.12 ± 4.76	12.38 ± 5.21	13.14 ± 5.52	13.58 ± 5.71
DMR 3	100	5.79 ± 2.37	12.28 ± 5.05	13.16 ± 5.44	14.18 ± 5.88	15.10 ± 6.35
	150	5.80 ± 2.39	12.50 ± 5.12	13.26 ± 5.44	14.32 ± 5.87	15.78 ± 6.52

	50	6.06 ± 2.92	9.04 ± 3.78	10.82 ± 4.42	11.38 ± 4.65	11.94 ± 4.88
DMR 4	100	5.57 ± 2.33	9.50 ± 4.00	11.12 ± 4.55	11.62 ± 4.76	12.16 ± 4.97
	150	5.48 ± 2.34	9.54 ± 3.95	11.18 ± 4.57	11.90 ± 4.86	12.20 ± 4.98

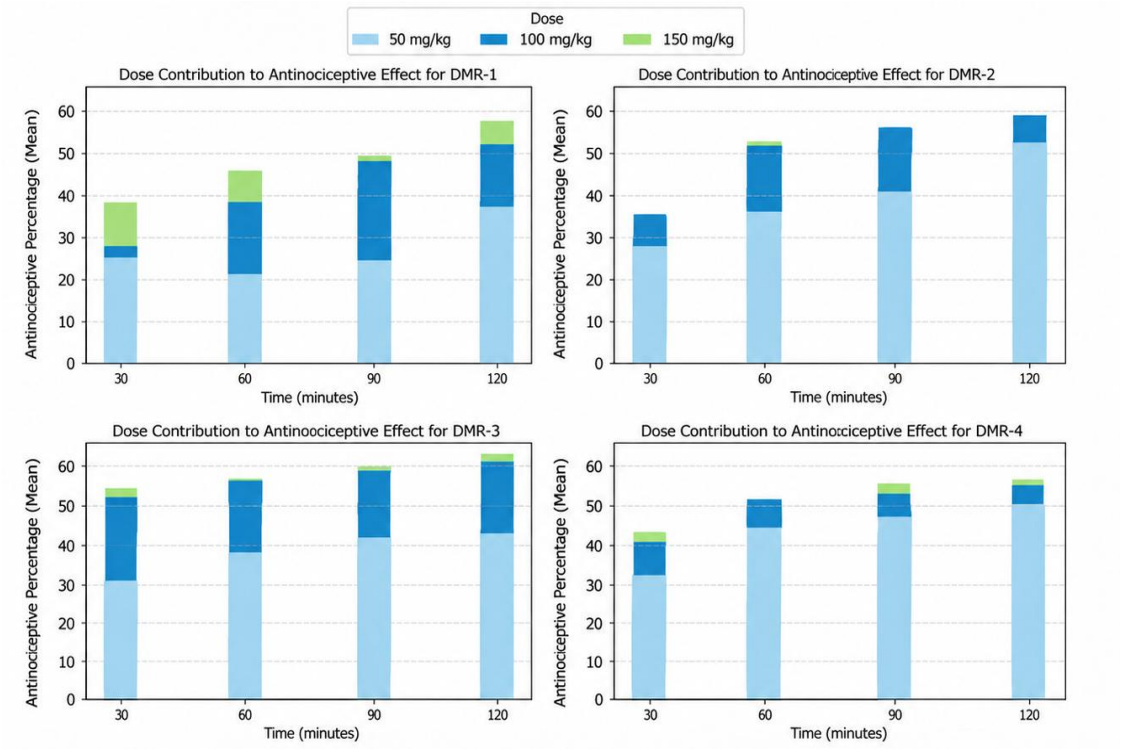


Figure 6. Dose–response relationship.

Statistical Analysis

The statistical analysis comparing the percentage of antinociception between DMR-1, DMR-2, DMR-3, DMR4, vehicle (negative control) and morphine (positive control) can be seen in Table S7a–l of the Supporting Information. Figure 7 shows the statistical analysis comparing the antinociceptive effect of each natural compound (DMR 1–4) at each dose level with the positive and negative controls. Each column represents a different dose, whereas each row represents a specific time interval. Horizontal bars indicate groups with statistically significant differences. An asterisk denotes significance at $p < 0.05$, two asterisks denote $p < 0.01$, and three asterisks denote $p < 0.001$. A box plot displays the median, minimum, maximum, and variance for each group.

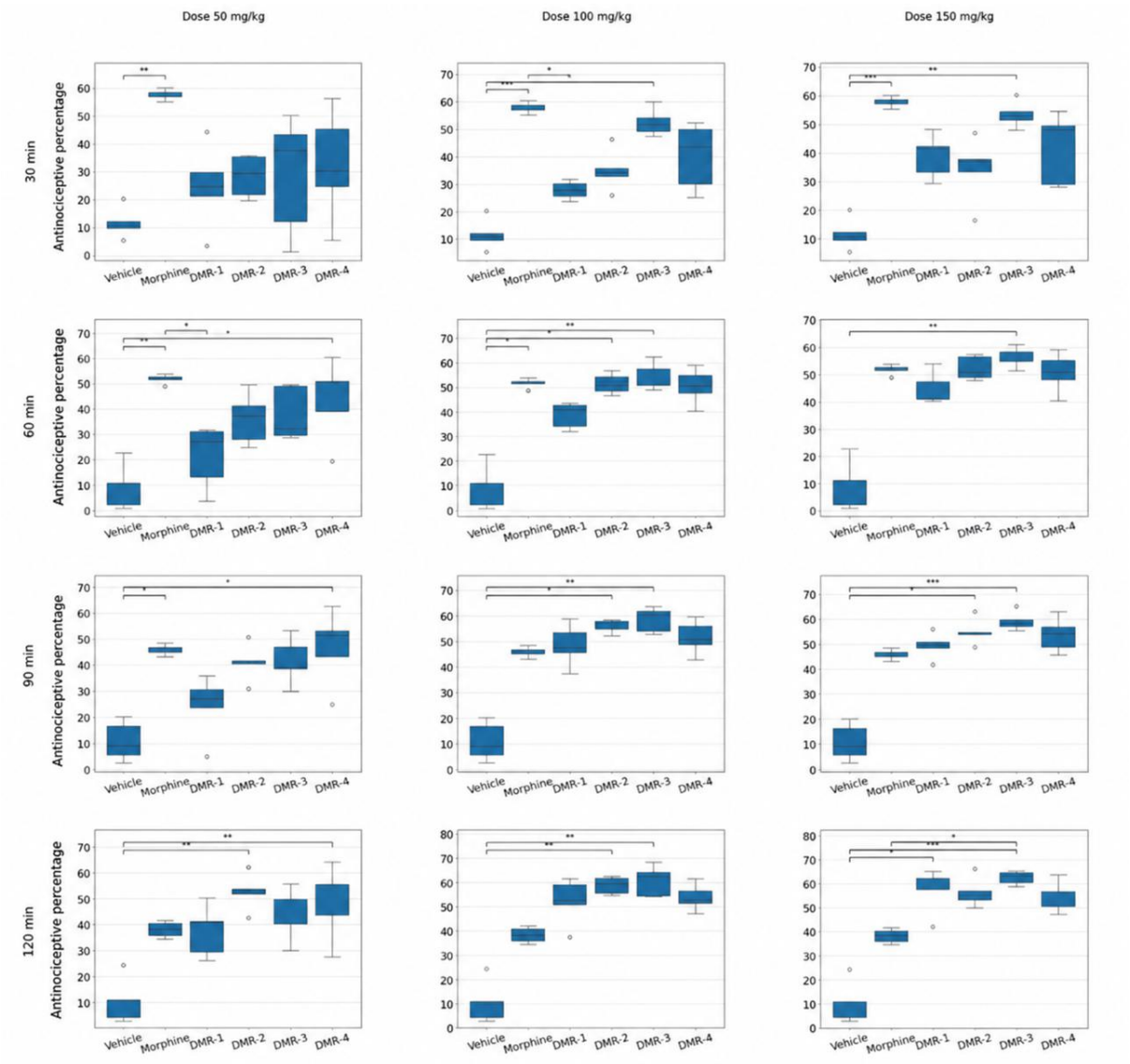


Figure 7. Results of the statistical analysis.

3. Discussion

In this work, computational techniques were applied for the prioritization of flavonoids with potential antinociceptive activity. While the model is not optimal, it allows exploration of the relationship between molecular structure of μ-opioid receptor-binding affinity and provides a quantitative framework for prioritizing structurally related natural compounds for experimental evaluation.

Multiple linear regression was selected because it provides an explicit relationship between molecular descriptors and the biological endpoint, allowing the contribution of the selected descriptors to be examined. Furthermore, this approach is widely used in QSAR studies [21–23] and is supported by the validation procedures, in accordance with OECD guidelines, that are implemented in QSARINS [24,25].

The model exhibits an R^2 of 0.7587, indicating a good fit to the experimental receptor-binding affinity data, and an adjusted R^2 of 0.7498, suggesting that the selected descriptors are suitable for fitting the model.

The LOF parameter of 0.5902 is low, suggesting no overfitting in the model with eight predictor variables. According to the low Kxx value (0.3093), the correlation between the model descriptors is low, so it can be assumed that there is no redundant information in the selected descriptors. The correlation matrix between the model descriptors is shown

in Table S5 of the Supporting Information. Furthermore, the correlation between the descriptors and the modeled response is adequate, according to the Delta K parameter (0.0433), with a small error in the training calculations and parameter estimation ($RMSE_{TS}$ = 0.7136; MAE_{TS} = 0.5694; s = 0.7283). As can be seen in Figure 2a, most of the observations in the training set (yellow dots) are close to the main diagonal (line y = x).

According to the validation exercises performed, the internal validation results demonstrate the stability of the model under the applied resampling procedures. The variance explained in the predictions using LOO and LMO yielded Q^2_{LOO} = 0.7346 and Q^2_{LMO} = 0.7316, respectively, which are comparable to the model's R^2 (0.7587), supporting the robustness of the model under internal perturbation. Figure 3a shows the predictions obtained through LOO validation. Considering that the dataset is sufficiently large, the perturbation of a single compound does not significantly affect the model fit. Similarly, when 30% of the data were excluded in the LMO procedure, comparable results were obtained. The Q^2_{LMO} values across the different iterations (red dots in Figure 3b) in relation to the correlation between the descriptors and the pKi (Kxy) were close to the model's Q^2 value (blue dots), further supporting the stability of the model under the applied LMO perturbations.

To demonstrate that the model is not the result of a random correlation, the y-scrambling procedure was employed by randomly assigning response values to the molecular descriptors. As expected, model performance decreases substantially, yielding $R^2_{Y\text{-}scr}$ = 0.0356 and $Q^2_{Y\text{-}scr}$ = −0.0474. These values are markedly lower than those obtained with the original model, indicating that the observed structure–activity relationship is unlikely to result from chance correlation. Figure 3c shows the $R^2_{Y\text{-}scr}$ and $Q^2_{Y\text{-}scr}$ values compared to the model's R^2 and Q^2 values.

External validation was performed using an independent prediction set not involved in the model development. The model yielded R^2_{PS} = 0.6895, Q^2-F1 = 0.6842, Q^2-F2 = 0.6838, and Q^2-F3 = 0.6378, with $RMSE_{PS}$ = 0.8743, MAE_{PS} = 0.6816, and CCC_{PS} = 0.8258, supporting its ability to predict the μ-opioid receptor-binding affinity of external compounds. Furthermore, the classical Golbraikh and Tropsha validation criteria were largely satisfied, with regression slopes (k = 0.9935 and k′ = 0.9947) close to unity and a difference between R^2_0 and R'^2_0 of 0.0720. The relative deviations from the origin-constrained regression coefficients were 0.0067 and 0.1111, respectively, indicating a slight deviation from the strict threshold in one regression orientation. The average r^2m value was 0.5708, with a Δr^2m of 0.1443, supporting acceptable agreement between experimental and predicted values according to these complementary validation parameters.

As shown in Figure 2a, compound 24 (apigenin) from the external prediction set (blue dots) was the observation furthest from the identity line and exhibited a large residual of 5.6546 (Figure 2b). The applicability domain analysis also identified this compound as an outlier. Therefore, its predictions should be interpreted with caution. To further assess its influence on external predictive performance, an additional analysis was conducted excluding this compound. The resulting R^2_{PS} increased to 0.7517, while RMSEext and MAE_{PS} decreased to 0.7646 and 0.6402, respectively. The CCC_{PS} also increased to 0.8644. Furthermore, the average r^2m increased to 0.6514, with a Δr^2m of 0.1096. The regression slopes (k = 1.0001 and k′ = 0.9909) remained close to unity, and both relative deviations from the origin-constrained regression coefficients were below 0.1. These findings indicate improved agreement between experimental and predicted values when considering compounds within the model's applicability domain.

Although the model demonstrated satisfactory internal and external validation performance, its predictive reliability should be restricted to compounds falling within its applicability domain. The Williams plot (Figure 3d), based on leverage values and stand-

ardized residuals, shows that compound 19 (tramadol) from the training set and compound 24 (apigenin) from the prediction set fall outside the applicability domain. Additionally, compound 23 (luteolin) from the training set exceeds the leverage threshold, although it is well predicted. This finding may be associated with the limited representation of flavonoids in the chemical space of the dataset. Consequently, predictions for compounds outside the applicability domain should be interpreted with caution, regardless of their individual prediction errors.

Finally, the model was used to predict the μ-opioid receptor-binding affinity of *B. purpurascens* flavonoids DMR1–4 at μ-receptors. Compound DMR2 is predicted in the highly potent category; compounds DMR1, DMR3 and aglycone in the potent category and compound DMR4 in the moderately potent category. These predictions suggest differences in receptor-binding affinity among the structurally related flavonoids and are consistent with the possibility that the glycosidic substituent contributes to their predicted molecular properties. However, the small number of compounds does not allow a general structure–activity relationship for glycosylation to be established. Although all compounds show predicted pKi values above seven, comparable to the range of reported μ-opioid receptor-binding affinities of some opioid compounds, only DMR1–3 is located in the chemical space where predictions are reliable.

The selection of the morphine dose (7.5 mg/kg, i.p.) was based on previously reported experimental studies [26], which provided a pharmacological reference for the positive control in the hot plate test. In contrast, the flavonoids were evaluated at higher doses (50, 100, and 150 mg/kg) because they are naturally occurring glycosylated compounds, for which oral absorption may be limited. Therefore, higher doses were considered appropriate for the preliminary characterization of their antinociceptive effects. However, these differences in administered doses do not allow direct comparisons of relative potency between morphine and the flavonoids.

The administration routes were selected considering the different pharmacological and ethnobotanical contexts of the compounds. Morphine was administered intraperitoneally, a parenteral route commonly used for its administration in the experimental and clinical context considered in this study. Conversely, the flavonoids were administered orally because they were isolated from *Boldoa purpurascens*, a plant traditionally used in popular medicine as a leaf decoction. Thus, oral administration was considered a relevant approach for the preliminary evaluation of these natural products in relation to their traditional use. Consequently, the comparison between morphine and flavonoids must be interpreted descriptively rather than as evidence of differences in intrinsic pharmacological potency.

When studying the sensitivity of mice to thermal pain with a dose of 50 mg/kg in the hot plate test, it was observed that at 30 min there were only significant differences between morphine and the vehicle ($p = 0.002$), and the antinociceptive effects of flavonoids were lower than that of morphine. After 60 min, differences were found between the vehicle and morphine ($p = 0.001$) and between the vehicle and DMR4 ($p = 0.038$). However, at 120 min, the activity of morphine decreased and was not significantly different from that of the vehicle, but differences were found between the vehicle and DMR4 ($p = 0.010$) and DMR2 ($p = 0.002$). These results suggest that at doses of 50mg/kg only compound DMR4 after 60 min and compound DMR2 after 120 min have significant antinociceptive effects relative to the vehicle, although they do not reach the observed response of morphine at the corresponding time points.

At a dose of 100 mg/kg, significant differences were found between the vehicle and morphine up to 60 min into the study ($p = 0.034$). However, the antinociceptive response of morphine decreases over time, as can be seen in Figure 5, where no differences are observed with the vehicle from 90 min of the study (Figure 7). In addition, compound

DMR3 showed significant antinociceptive activity from 30 min ($p = 0.006$) and DMR2 from 60 min ($p = 0.048$), reaching values within the range of the response observed for morphine at selected time points.

At a dose of 150 mg/kg, similar results were obtained to those at a dose of 100 mg/kg. The results for compound DMR3 were consistent from 30 min ($p = 0.008$), and compound DMR1 also achieved significant antinociceptive activity relative to the vehicle at this dose after 120 min ($p = 0.021$). The results suggest that the compound with the most consistent antinociceptive profile is DMR3 at doses between 100 and 150 mg/kg.

In general, morphine exhibits high levels of antinociception after 30 min of study, which decrease over time, as shown in Figure 5. However, flavonoid activity increases over time. This difference in temporal profiles may reflect, among other factors, the different routes of administration used for the reference drug and flavonoids. Because morphine was administered intraperitoneally and the flavonoids orally, the present study does not allow pharmacokinetic mechanisms underlying these differences to be established.

The delayed increase in antinociceptive activity observed for some flavonoids may be associated with their oral absorption and possible metabolic transformation, particularly considering that flavonoid glycosides generally exhibit poor oral absorption. In this context, it remains unclear whether the observed effects result from the direct interaction of the parent compounds with μ-opioid receptors or involve active metabolites generated following oral administration. Although the QSAR model predicts potential μ-opioid receptor affinity, the relationship between this prediction and the observed in vivo antinociceptive activity remains to be elucidated. Thus, both direct receptor interaction and a potential prodrug-like contribution of flavonoid metabolism represent plausible mechanisms that warrant further investigation.

Based on these results, the recommended dose for achieving a good antinociceptive activity profile of the flavonoids DMR1–4 was analyzed. Figure 6 shows that only compound DMR1 exhibits a notable increase in activity when the dose is increased to 150 mg/kg. However, this compound shows lower activity compared to DMR2 and DMR3 at 100 mg/kg.

The comparison between morphine and the flavonoids should therefore be interpreted descriptively rather than as a direct comparison of potency, because the compounds differed in both dose and route of administration. In addition, the relatively large standard deviations observed in some DMR-treated groups indicate considerable interindividual variability in the antinociceptive response. Therefore, statistically significant differences should be interpreted cautiously, considering both the magnitude of the observed effects and the variability within each group, because statistical significance does not necessarily imply a robust or reproducible treatment effect. Overall, the in vivo findings provide pharmacological support for the computational prioritization strategy, particularly for DMR3. However, the present data do not establish that the observed antinociceptive effects are mediated specifically through μ-opioid receptors. Additional receptor-level pharmacological studies, such as binding assays or antagonist-based mechanistic experiments, would be required to establish this relationship.

4. Materials and Methods

4.1. In Silico Assay

In order to correlate the chemical structure of μ-opioid receptor ligands with their experimentally determined receptor-binding affinity, a mathematical model was developed. Once validated, it was used to prioritize flavonoids isolated from *Boldoa purpurascens* for subsequent experimental evaluation.

4.1.1. Dataset

The dataset was composed from experimental studies published in the scientific literature [27–47]. The SMILES codes for each molecule in the dataset can be consulted in Table S1 of the Supporting Information. Peptides and racemic compounds were excluded. The dataset consists of 300 molecules with reported μ-opioid receptor binding constants (Ki (nM)), expressed as pKi [−log Ki (M)], whose values were used as the response variable representing μ-opioid receptor-binding affinity.

The compounds are structurally diverse and include FDA-approved opioid drugs for pain management, as well as experimental compounds derived from benzomorphan, nitrazines (synthetic benzimidazole opioids), 4-alkyl-1-oxa-4,9-diazaspiro [5.5]undecane, aryl-naloxamide, 5-pyrrolidinylquinoxalines, and phenylimidazoles, among others. The most representative structural scaffolds of the data are shown in Figure 8.

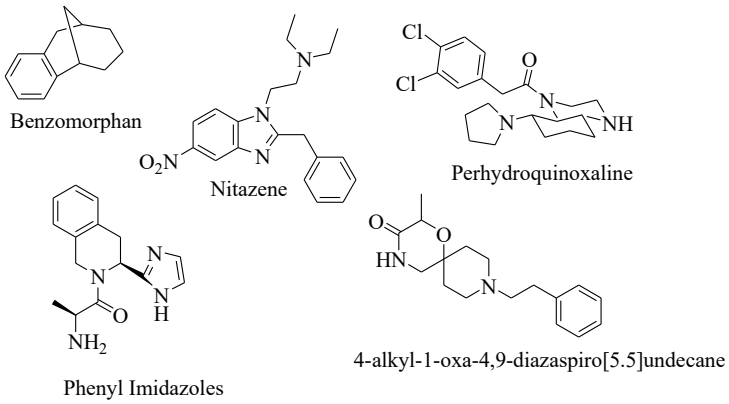


Figure 8. Structural scaffolds of the dataset.

4.1.2. Molecular Descriptors

The 0D-3D molecular descriptors and fingerprints implemented in the Dragon software (Kode srl. v.7.0) [48] were calculated, starting from a structural representation of the molecules previously optimized, with the semi-empirical method AM1. Constant, near-constant, and correlation descriptors greater than 95% were eliminated, as they were considered redundant for subsequent modeling.

4.1.3. Pre-Processing

Given that the compounds come from different bibliographic sources and the structural diversity shown in the data, a hierarchical cluster analysis was developed in Python 3.10 for data exploration and preliminary analysis. This method is useful for identifying duplicate compounds (compounds that are joined at a distance of zero) and potential outliers (compounds that are joined at a very large distance from the rest of the database). From each cluster observed in the dendrogram, the database was divided into a training set (75% of each cluster) and a prediction set (25% of each cluster), ensuring structural representativeness in both groups.

4.1.4. Modeling

For the development of the model, the QSARINS software (QSAR-INSubria v. 2.2.4) [25] was used, based on the experience of the QSAR Research Unit of Insubria, which allows the development of Multiple Linear Regression (MLR) models, by Ordinary Least Squares (OLS), according to Equation (2).

$$Y_i = b_0 + \sum_{j=1}^{n} b_j x_{ij} + e_i \quad (2)$$

where a linear relationship was calculated between the studied responses Y_i and the selected values of the descriptors K_{ij}; e_i is the random error (also called the model residual). The intersection b_0 and the coefficients b_j therefore must be estimated.

Models with sizes ranging from one to ten variables were generated using a genetic algorithm [49] for variable selection, with 10,000 iterations. For the selection of the best model, Ockham's razor was considered, as well as the following criteria: fit (highest R^2), robustness (highest Q^2_{LMO}), stability (lowest R^2-Q^2_{LMO}), low correlation of descriptors (low K_{XX}), high correlation with the response (high dK), and the root mean square error of (a) training calculation ($RMSE_{TS}$), (b) training prediction in cross-validation ($RMSE_{CV}$), and (c) external prediction series ($RMSE_{PS}$).

4.1.5. Validation

The resulting model was validated, assessing its applicability domain (AD) and predictive power, according to the OECD regulatory principles [50–52]. To comply with principle 1, the μ-opioid receptor binding constant (Ki) was used as the activity measurement point, as previously specified.

Principle 2 was considered in the selection of the training algorithm. In this case, a linear algorithm was used, relating to the chemical structure descriptors and the activity endpoint through a knowledge-based mathematical equation developed by experts.

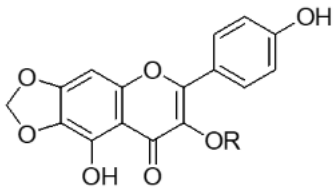
To define AD (principle 3), the William chart was used, considering that reliable model predictions have leverage values below the critical leverage within ± 3 standard deviations. Compounds outside these limits were considered to have predictions of reduced reliability and were not interpreted as reliable model-based predictions.

According to Principle 4, model fit was evaluated considering the coefficient of determination (R^2) and the modified R^2adj, which also assesses the effectiveness of adding a new descriptor to the model. Furthermore, internal validation exercises were performed to verify the stability and robustness of the model. First, a leave-one-out (LOO) cross-validation was developed, followed by leave-many-out (LMO) validation, iteratively removing 30% of the data until 2000 iterations were completed. To demonstrate that the model was not the result of a chance correlation, the y-scrambling procedure was applied, randomly assigning responses so that there was no correlation with the descriptors. Consequently, the model's performance was expected to decrease drastically. Once the models were internally validated and the possibility of a chance correlation was ruled out, external validation was performed to verify their ability to predict new compounds, or their predictive power. The procedure was carried out by applying the model function obtained from the training set to the prediction set.

4.1.6. Virtual Screening

The validated QSAR-RLM model obtained was used to predict the μ-opioid receptor-binding affinity of four naturally occurring flavonoids (DMR 1–4) isolated from the leaves of the plant *Boldoa purpurascens* Cav. Their extraction, isolation, purification, and structural characterization procedures, including electrospray ionization mass spectrometry (ESI-MS) and one- and two-dimensional nuclear magnetic resonance (1D and 2D NMR) spectroscopy, were previously reported by González-Mosquera et al. (2008) [19]. The molecular structures of the evaluated flavonoids are shown in Figure 9. In addition, the gomphrenol aglycone of these flavonoids was included in the in silico study, since this compound could potentially be generated following hydrolysis of the glycosidic moiety; however, this metabolic transformation was not experimentally assessed in the present study.

Following the study by Volpe et al. [47], three categories were used to characterize the studied molecules, which are summarized as follows: high potency Ki ≤ 1 nM (pKi ≥ 9), potent 1 < Ki < 100 (7 < pKi < 9), and moderately potent Ki ≥ 100 nM (pKi ≤ 7).



Aglycone	R = H
DMR1	R = β-D-Xyl(2←1)-α-L-Rha
DMR2	R = β-D-Glc
DMR3	R = β-D-Glc(2←1)-α-L-Rha
DMR4	R = β-D-Xyl

Figure 9. Chemical structure of the DMR 1–4 flavonoids from *Boldoa purpurascens*.

4.2. In Vivo Assay

To determine the in vivo antinociceptive activity of the studied flavonoids, the hot plate test [53] was used. This method is widely used in pain research to evaluate the response of animals to a controlled thermal stimulus and is primarily used to assess centrally acting analgesics.

4.2.1. Reagents

The reagents used in the different experiments were Tween 80 (UNICHEM, Quito, Ecuador), morphine (Sigma-Aldrich, Darmstadt, Germany), and flavonoids obtained from *Boldoa purpurascens* by researchers from the Department of Pharmacy at the Central University of Las Villas (DMR 1, DMR 2, DMR 3, DMR 4).

4.2.2. Biological Model

NMRI mice of both sexes from the National Center to Produce Laboratory Animals, Havana, Cuba (CENPALAB), was used, along with their corresponding Certificate of Quality.

4.2.3. Experimental Conditions

The animals were provided by CENPALAB. They were kept for seven days to acclimatize, with ambient temperature, relative humidity of 60 ± 5%, and 12-h light/12-h dark cycles. They received controlled feeding (EMO 1002 concentrated feed in pellet form with its corresponding Quality Certificate issued by CENPALAB and potable water *ad libitum*. They were housed in polyethylene cages with metal mesh, each cage housing five animals per cage. They were deprived of food 18 h before the start of the experiment and of water one hour before.

4.2.4. Experimental Procedure

A total of 70 NMRI mice were randomly allocated to 14 experimental groups (n = 5 per group), each consisting of three males and two females. The groups included a negative control receiving the vehicle alone (10 mL/Kg, p.o.), a positive reference control treated with morphine (7.5 mg/kg, i.p.), and 12 experimental groups receiving the flavonoids DMR 1–4 at three dose levels (50, 100, and 150 mg/kg, p.o.). The flavonoids were administered orally in a volume of 0.25 mL using a vehicle composed of Tween 80, ethanol, and water in a 2:2:20 ratio. No sex-stratified statistical analysis was performed because of the limited sample size within each sex.

The experimental design aimed to characterize the antinociceptive responses induced by the evaluated flavonoids rather than to establish dose-equivalent comparisons

with morphine. Therefore, differences between morphine and the flavonoids were interpreted descriptively and were not considered indicative of relative pharmacological potency.

The hot plate test was performed at 55 ± 1 °C, with a maximum exposure time (cut-off) of 30 s to prevent thermal tissue injury. Animals were removed from the heated surface when they exhibited a predefined nociceptive response (hind paw licking or jumping) or reached the maximum exposure time. Before treatment, two baseline reaction time measurements were recorded at 10-min intervals, and their average was defined as the pre-treatment reaction time (Tb). Following compound administration, reaction times were measured at 30-min intervals over a 120-min period. These measurements were defined as post-treatment reaction times (Ta). The mean reaction time was calculated for each experimental group, and the percentage of analgesia was determined using Equation (3).

$$\text{Antinociceptive Score}(\%) = \frac{T_a - T_b}{T_a} * 100 \quad (3)$$

where T_b is the reaction time (in second) before drug administration; T_a is the reaction time (in second) after drug administration.

4.2.5. Statistical Analysis

The statistical analysis was performed using the Python 3.10 statistical library. A descriptive analysis was conducted for each group, considering the mean, minimum, maximum, 25, 50, and 75 percentile values, as well as the dispersion per group. To compare the percentages of analgesia between the different groups, the non-parametric Kruskal–Wallis test was performed. This test was used to assess whether there were overall differences between the groups without assuming the requirements of normality or homogeneous variances, using a significance level of $p < 0.05$. To specifically determine which pairs of groups differed from each other, a post-hoc comparison was performed using Dunn's test with Bonferroni correction, controlling for Type I error of multiple comparisons by adjusting the significance level.

4.2.6. Euthanasia

Euthanasia was performed 24 h after completion of the experimental procedures by cervical dislocation, following the recommendations of the AVMA Guidelines for the Euthanasia of Animals (2020) [54]. The procedure was performed by an experienced specialist after prior anesthesia with diethyl ether, in accordance with the institutional protocol in place at the time of the study.

5. Conclusions

The combined computational and experimental findings support the use of QSAR models as prioritization tools in natural-product research. The developed MLR model explained more than 75% of the variance in μ-opioid receptor-binding affinity within the training set and showed satisfactory internal and external predictive performance. Its predictions should therefore be interpreted within the defined applicability domain. The model allowed the computational prioritization of four flavonoids isolated from *Boldoa purpurascens*, which showed favorable predicted μ-opioid receptor-binding-affinity profiles. Among them, DMR3 exhibited the most consistent antinociceptive effect, particularly at doses of 100 and 150 mg/kg. However, the differences observed in comparison with morphine should be interpreted cautiously because the treatments differed in both dose and route of administration. Consequently, the present findings do not establish the

relative potency of the flavonoids compared with morphine or demonstrate that their antinociceptive effects are mediated specifically through μ-opioid receptors. The differences observed among the studied flavonoids, despite their structural similarity, suggest that glycosylation may contribute to differences in antinociceptive activity. Nevertheless, this hypothesis requires further investigation using a larger series of structurally related compounds and additional pharmacological studies.

Supplementary Materials: The following supporting information can be downloaded at: https://www.mdpi.com/article/10.3390/molecules31234364/s1, Table S1: SMILES codes for the database molecules. Table S2: Definition of the selected molecular descriptors. Table S3: Experimental and predicted values by the MLR model for the training set. Table S4: Experimental and predicted values by the MLR model for the prediction set. Table S5: Correlation matrix between the model descriptors. Table S6: Recording of pain behavioral responses and determination of the percentage of analgesia by group, stratified by dose and time elapsed since administration. (DMR-1, DMR-2, DMR-3, DMR4, Vehicle (negative control) and Morphine (positive control). Table S7: Statistical analysis comparing de analgesia percentage between DMR-1, DMR-2, DMR-3, DMR4, Vehicle (negative control) and Morphine (positive control).

Author Contributions: Conceptualization, D.M.G.-M. and A.L.-S.; Methodology, D.M.G.-M., A.L.-S., S.J. and Y.C.-C.; Software, Y.C.-C.; Formal analysis, R.D.-A.; Investigation, D.M.G.-M., A.L.-S., I.F.-G. and Y.C.-C.; Resources, D.M.G.-M., A.O.-M. and A.L.-S.; Data curation, R.D.-A. and Y.C.-C.; Writing—original draft preparation, Y.C.-C. and R.D.-A.; Writing—review and editing, D.M.G.-M., I.F.-G., R.D.-A., A.O.-M., S.J., E.T., I.F.-G. and Y.C.-C.; Supervision, D.M.G.-M., A.O.-M., E.T.; Funding acquisition, A.O.-M. All authors have read and agreed to the published version of the manuscript.

Funding: This research was financially supported by the Pharmacy Department from Central University of Las Villas. The article processing charge (APC) was funded by the Open Access Publishing Fund of the University of Bayreuth. This research received funding from the Emmy Noether Programme of the German Research Foundation DFG (Grant number: OS 497/6-1, AOBJ: 704122).

Institutional Review Board Statement: Ethical approval for this study was obtained from the ethics commission of the Faculty of Chemistry and Pharmacy of the Central University "Marta Abreu" of Las Villas on 15 November 2024. All researchers respected the ethical principles governing animal experimentation, complying with established Bioethics and Biosafety Standards [55].

Data Availability Statement: The database used in this study, as well as the results generated, are available in the Supplementary Materials

Acknowledgments: Y.C.-C. thanks Paola Gramatica for providing a free academic license of the QSARINS software. Authors acknowledge funding by the Open Access Publishing Fund of the University of Bayreuth.

Conflicts of Interest: The authors declare no conflicts of interest.

Abbreviations

AD	Applicability Domain
AM1	Austin Model 1
h	Leverage
h*	Critical leverage
Ki	μ-opioid receptor binding constant
LMO	Leave Many Out
LOO	Leave One Out
MLR	Multiple Linear Regression
OECD	Organization for Economic Cooperation and Development

OLS	Ordinary Least Square
PS	Prediction Set
Q^2	Cross-validated coefficient
QSAR	Quantitative Structure–Activity Relationship
R^2	Coefficient of Determination
Ta	Reaction time after drug administration
Tb	Reaction time before drug administration
TS	Training Set

References

1. García-Domínguez, M. Enkephalins and Pain Modulation: Mechanisms of Action and Therapeutic Perspectives. *Biomolecules* **2024**, *14*, 926. https://doi.org/10.3390/biom14080926.
2. van Rensburg, R.; Reuter, H. An overview of analgesics: NSAIDs, paracetamol, and topical analgesics Part 1. *S. Afr. Fam. Pract.* **2019**, *61*, S4–S10. https://doi.org/10.1080/20786190.2019.1610228.
3. Andrew, F. Chronic Pain and Its Impact on Quality of Life: A Comprehensive Review. Available online: https://www.hilarispublisher.com/open-access/chronic-pain-and-its-impact-on-quality-of-life-a-comprehensive-review-107453.html (accessed on 14 May 2026).
4. Shimoji, K.; Fujioka, H. Pharmacology of Analgesics. In *Chronic Pain Management in General and Hospital Practice*; Shimoji, K., Nader, A., Hamann, W., Eds.; Springer: Singapore, 2021; pp. 55–86.
5. Pasternak, G.W. Opiate Pharmacology and Relief of Pain. *J. Clin. Oncol.* **2014**, *32*, 1655–1661. https://doi.org/10.1200/JCO.2013.53.1079.
6. Jayakar, S.; Shim, J.; Jo, S.; Bean, B.P.; Singeç, I.; Woolf, C.J. Developing nociceptor-selective treatments for acute and chronic pain. *Sci. Transl. Med.* **2021**, *13*, eabj9837. https://doi.org/10.1126/scitranslmed.abj9837.
7. Amine, S.; Montembault, A.; Fumagalli, M.; Osorio-Madrazo, A.; David, L. Controlled Polyelectrolyte Association of Chitosan and Carboxylated Nano-Fibrillated Cellulose by Desalting. *Polymers* **2021**, *13*, 2023. https://doi.org/10.3390/polym13122023.
8. Roig y Mesa, J.T. *Plantas Medicinales Aromáticas o Venenosas de Cuba*; 2nd ed.; Editorial Científico-Técnica: La Habana, Cuba, 2015; Volume 2, ISBN 978-959-05-0809-7.
9. Apak, R.; Güçlü, K.; Demirata, B.; Ozyürek, M.; Celik, S.E.; Bektaşoğlu, B.; Berker, K.I.; Ozyurt, D. Comparative evaluation of various total antioxidant capacity assays applied to phenolic compounds with the CUPRAC assay. *Molecules* **2007**, *12*, 1496–1547. https://doi.org/10.3390/12071496.
10. Ebunang, D.V.T.; Tajeu, K.Y.; Pecheu, C.N.; Jiokeng, S.L.Z.; Tamo, A.K.; Doench, I.; Osorio-Madrazo, A.; Tonle, I.K.; Ngameni, E. Amino-Functionalized Laponite Clay Material as a Sensor Modifier for the Electrochemical Detection of Quercetin. *Sensors* **2022**, *22*, 6173. https://doi.org/10.3390/s22166173.
11. González Mosquera, D.M.; Cañizares Carmenate, Y.; Rivero Arbolay, A.I.; Romero Borges, R.; García Gómez, M.L.; Blanco Machado, F.; Valcarel, K.G.; Díaz-Amador, R.; Osorio-Madrazo, A.; Saez, G.C.; et al. Evaluation of the antihypertensive activity of the aqueous extract and the major flavonoid from *Boldoa purpurascens* cav. leaves. *Fitoterapia* **2025**, *185*, 106724. https://doi.org/10.1016/j.fitote.2025.106724.
12. Cañizares-Carmenate, Y.; González-Mosquera, D.M.; Perera-Sardiña, Y.; Hernández-Rodríguez, E.W.; Díaz-Amador, R.; Castillo-Garit, J.A.; Tuenter, E. Natriuretic effect of 4′,5-dihydroxy-6,7-methylenedioxyflavonol-3-O-α-L-rhamnopyranosyl-(1→2)-β-D-xylopyranoside from Boldoa purpurascens: In silico and in vivo studies. *J. Biomol. Struct. Dyn.* **2026**, *44*, 416–426. https://doi.org/10.1080/07391102.2024.2426075.
13. Ortega, Y.H.; Foubert, K.; Berghe, W.V.; Chirumamilla, C.S.; Pieters, L.; Mosquera, D.M.G.; Apers, S. Flavonol glycosides from the leaves of *Boldoa purpurascens* and their anti-inflammatory properties. *Phytochem. Lett.* **2017**, *19*, 71–76. https://doi.org/10.1016/j.phytol.2016.12.002.
14. Domínguez-Oliva, A.; Hernández-Ávalos, I.; Martínez-Burnes, J.; Olmos-Hernández, A.; Verduzco-Mendoza, A.; Mota-Rojas, D. The Importance of Animal Models in Biomedical Research: Current Insights and Applications. *Animals* **2023**, *13*, 1223. https://doi.org/10.3390/ani13071223.
15. Chang, M.C.J.; Grieder, F.B. The continued importance of animals in biomedical research. *Lab Anim.* **2024**, *53*, 295–297. https://doi.org/10.1038/s41684-024-01458-4.
16. Kiani, A.K.; Pheby, D.; Henehan, G.; Brown, R.; Sieving, P.; Sykora, P.; Marks, R.; Falsini, B.; Capodicasa, N.; Miertus, S.; et al. Ethical considerations regarding animal experimentation. *J. Prev. Med. Hyg.* **2022**, *63*, E255. https://doi.org/10.15167/2421-4248/jpmh2022.63.2S3.2768.

17. Shaker, B.; Ahmad, S.; Lee, J.; Jung, C.; Na, D. In silico methods and tools for drug discovery. *Comput. Biol. Med.* **2021**, *137*, 104851. https://doi.org/10.1016/j.compbiomed.2021.104851.
18. Ouma, R.B.O.; Ngari, S.M.; Kibet, J.K. A review of the current trends in computational approaches in drug design and metabolism. *Discov. Public Health* **2024**, *21*, 108. https://doi.org/10.1186/s12982-024-00229-3.
19. Mosquera, D.M.G.; Kilonda, A.; Toppet, S.; Compernolle, F.; Dehaen, W.; François, I.E.J.A.; Cammue, B.P.A.; Apers, S.; Pieters, L.; Cuéllar, A.C. New Flavonoids from *Boldoa purpurascens* Cav. *Planta Med.* **2008**, *74*, 1468–1473. https://doi.org/10.1055/s-2008-1081332.
20. Atkinson, A.C. *Plots, Transformations, and Regression: An Introduction to Graphical Methods of Diagnostic Regression Analysis*; Oxford Statistical Science Series; Oxford University Press: Oxford, NY, USA, 1987.
21. Das, N.R.; Achary, P.G.R. Quantitative Structure–Activity Relationships (QSARs) Study for KCNQ Genes (Kv7) and Drug Discovery. In *Advances in Intelligent Computing and Communication: Proceedings of ICAC 2020*; Springer: Singapore, 2021; pp. 61–70.
22. Cañizares-Carmenate, Y.; Díaz-Amador, R.; Castillo-Garit, J.A. Exploring MD-LOVIs, DIVATI and DRAGON descriptors for thermolysin inhibition modeling. *Lett. Drug Des. Discov.* **2026**, *23*, 100380. https://doi.org/10.1016/j.lddd.2026.100380.
23. Prabha, T.; Saravanan, T.; Heera, G.; Prakash, S.; Latha, S.; M.k, K.; M.v.n.l, C.; Sivakumar, T. Discovering a 4H-chromen-4-one Framework to Target Breast Cancer with a State-of-the-art QSAR Model. *Curr. Enzym. Inhib.* **2025**, *21*, 153–171. https://doi.org/10.2174/0115734080335471250320032842.
24. Cañizares-Carmenate, Y.; Campos Delgado, L.E.; Torrens, F.; Castillo-Garit, J.A. Thorough evaluation of OECD principles in modelling of 1-[(2-hydroxyethoxy) methyl]-6-(phenylthio) thymine derivatives using QSARINS. *SAR QSAR Environ. Res.* **2020**, *31*, 741–759.
25. Gramatica, P.; Chirico, N.; Papa, E.; Cassani, S.; Kovarich, S. QSARINS: A new software for the development, analysis, and validation of QSAR MLR models. *J. Comput. Chem.* **2013**, *34*, 2121–2132. https://doi.org/10.1002/jcc.23361.
26. Ahmadi, S.; Golbaghi, H.; Azizbeigi, R.; Esmailzadeh, N. N-methyl-D-aspartate receptors involved in morphine-induced hyperalgesia in sensitized mice. *Eur. J. Pharmacol.* **2014**, *737*, 85–90.
27. Srivastava, S.K.; Husbands, S.M.; Aceto, M.D.; Miller, C.N.; Traynor, J.R.; Lewis, J.W. 4′-Arylpyrrolomorphinans: Effect of a pyrrolo-N-benzyl substituent in enhancing δ-opioid antagonist activity. *J. Med. Chem.* **2002**, *45*, 537–540.
28. Journigan, V.B.; Polgar, W.E.; Khroyan, T.V.; Zaveri, N.T. Designing bifunctional NOP receptor–mu opioid receptor ligands from NOP-receptor selective scaffolds. Part II. *Bioorg. Med. Chem.* **2014**, *22*, 2508–2516.
29. Hayashi, S.; Nakata, E.; Morita, A.; Mizuno, K.; Yamamura, K.; Kato, A.; Ohashi, K. Discovery of {1-[4-(2-{hexahydropyrrolo[3,4-*c*]pyrrol-2(1*H*)-yl}-1*H*-benzimidazol-1-yl)piperidin-1-yl]cyclooctyl}methanol, systemically potent novel non-peptide agonist of nociceptin/orphanin FQ receptor as analgesic for the treatment of neuropathic pain: Design, synthesis, and structure–activity relationships. *Bioorg. Med. Chem.* **2010**, *18*, 7675–7699. https://doi.org/10.1016/j.bmc.2010.07.034.
30. García, M.; Virgili, M.; Alonso, M.; Alegret, C.; Farran, J.; Fernández, B.; Bordas, M.; Pascual, R.; Burgueño, J.; Vidal-Torres, A.; et al. Discovery of EST73502, a Dual μ-Opioid Receptor Agonist and σ1 Receptor Antagonist Clinical Candidate for the Treatment of Pain. *J. Med. Chem.* **2020**, *63*, 15508–15526. https://doi.org/10.1021/acs.jmedchem.0c01127.
31. Pasquinucci, L.; Prezzavento, O.; Marrazzo, A.; Amata, E.; Ronsisvalle, S.; Georgoussi, Z.; Fourla, D.-D.; Scoto, G.M.; Parenti, C.; Aricò, G.; et al. Evaluation of N-substitution in 6,7-benzomorphan compounds. *Bioorg. Med. Chem.* **2010**, *18*, 4975–4982. https://doi.org/10.1016/j.bmc.2010.06.005.
32. Klimas, R.; Mikus, G. Morphine-6-glucuronide is responsible for the analgesic effect after morphine administration: A quantitative review of morphine, morphine-6-glucuronide, and morphine-3-glucuronide. *Br. J. Anaesth.* **2014**, *113*, 935–944. https://doi.org/10.1093/bja/aeu186.
33. Neumeyer, J.L.; Peng, X.; Knapp, B.I.; Bidlack, J.M.; Lazarus, L.H.; Salvadori, S.; Trapella, C.; Balboni, G. New opioid designed multiple ligand from Dmt-Tic and morphinan pharmacophores. *J. Med. Chem.* **2006**, *49*, 5640–5643.
34. Webster, D.E.; He, Y.; Chen, S.-N.; Pauli, G.F.; Farnsworth, N.R.; Wang, Z.J. Opioidergic mechanisms underlying the actions of *Vitex agnus-castus* L. *Biochem. Pharmacol.* **2011**, *81*, 170–177. https://doi.org/10.1016/j.bcp.2010.09.013.
35. Greedy, B.M.; Bradbury, F.; Thomas, M.P.; Grivas, K.; Cami-Kobeci, G.; Archambeau, A.; Bosse, K.; Clark, M.J.; Aceto, M.; Lewis, J.W. Orvinols with mixed kappa/mu opioid receptor agonist activity. *J. Med. Chem.* **2013**, *56*, 3207–3216.
36. Eans, S.O.; Ganno, M.L.; Mizrachi, E.; Houghten, R.A.; Dooley, C.T.; McLaughlin, J.P.; Nefzi, A. Parallel synthesis of hexahydrodiimidazodiazepines heterocyclic peptidomimetics and their in vitro and in vivo activities at μ (MOR), δ (DOR), and κ (KOR) opioid receptors. *J. Med. Chem.* **2015**, *58*, 4905–4917.

37. Kozell, L.B.; Eshleman, A.J.; Wolfrum, K.M.; Swanson, T.L.; Schutzer, K.A.; Schutzer, W.E.; Abbas, A.I. Pharmacology of newly identified nitazene variants reveals structural determinants of affinity, potency, selectivity for mu opioid receptors. *Neuropharmacology* **2025**, *276*, 110512. https://doi.org/10.1016/j.neuropharm.2025.110512.
38. De Costa, B.R.; Iadarola, M.J.; Rothman, R.B.; Berman, K.F.; George, C.; Newman, A.H.; Mahboubi, A.; Jacobson, A.E.; Rice, K.C. Probes for narcotic receptor mediated phenomena. 18. Epimeric 6. alpha.-and 6. beta.-iodo-3, 14-dihydroxy-17-(cyclopropylmethyl)-4, 5. alpha.-epoxymorphinans as potential ligands for opioid receptor single photon emission computed tomography: Synthesis, evaluation, and radiochemistry of [125I]-6. beta.-iodo-3, 14-dihydroxy-17-(cyclopropylmethyl)-4, 5. alpha.-epoxymorphinan. *J. Med. Chem.* **1992**, *35*, 2826–2835.
39. Breslin, H.J.; Miskowski, T.A.; Rafferty, B.M.; Coutinho, S.V.; Palmer, J.M.; Wallace, N.H.; Schneider, C.R.; Kimball, E.S.; Zhang, S.-P.; Li, J. Rationale, design, and synthesis of novel phenyl imidazoles as opioid receptor agonists for gastrointestinal disorders. *J. Med. Chem.* **2004**, *47*, 5009–5020.
40. Cami-Kobeci, G.; Polgar, W.E.; Khroyan, T.V.; Toll, L.; Husbands, S.M. Structural determinants of opioid and NOP receptor activity in derivatives of buprenorphine. *J. Med. Chem.* **2011**, *54*, 6531–6537.
41. Hammami, S.; Mighri, Z.; Dooley, C.T.; Nefzi, A. Synthesis and analgesic activity of alkylated, reduced and constrained oligoheterocyclic peptidomimetic analogs of Leu-enkephalin. *Bioorg. Med. Chem. Lett.* **2014**, *24*, 4482–4485. https://doi.org/10.1016/j.bmcl.2014.07.090.
42. Majumdar, S.; Subrath, J.; Le Rouzic, V.; Polikar, L.; Burgman, M.; Nagakura, K.; Ocampo, J.; Haselton, N.; Pasternak, A.R.; Grinnell, S. Synthesis and evaluation of aryl-naloxamide opiate analgesics targeting truncated exon 11-associated μ opioid receptor (MOR-1) splice variants. *J. Med. Chem.* **2012**, *55*, 6352–6362.
43. Bourgeois, C.; Werfel, E.; Galla, F.; Lehmkuhl, K.; Torres-Gómez, H.; Schepmann, D.; Kögel, B.; Christoph, T.; Straßburger, W.; Englberger, W.; et al. Synthesis and pharmacological evaluation of 5-pyrrolidinylquinoxalines as a novel class of peripherally restricted κ-opioid receptor agonists. *J. Med. Chem.* **2014**, *57*, 6845–6860. https://doi.org/10.1021/jm500940q.
44. Nemoto, T.; Yamamoto, N.; Watanabe, A.; Fujii, H.; Hasebe, K.; Nakajima, M.; Mochizuki, H.; Nagase, H. Synthesis of 6, 14-epoxymorphinan derivatives and their pharmacologies. *Bioorg. Med. Chem.* **2011**, *19*, 1205–1221.
45. Ida, Y.; Matsubara, A.; Nemoto, T.; Saito, M.; Hirayama, S.; Fujii, H.; Nagase, H. Synthesis of quinolinomorphinan derivatives as highly selective δ opioid receptor ligands. *Bioorg. Med. Chem.* **2012**, *20*, 5810–5831.
46. Healy, J.R.; Bezawada, P.; Shim, J.; Jones, J.W.; Kane, M.A.; MacKerell, A.D.; Coop, A.; Matsumoto, R.R. Synthesis, modeling, and pharmacological evaluation of UMB 425, a mixed μ agonist/δ antagonist opioid analgesic with reduced tolerance liabilities. *ACS Chem. Neurosci.* **2013**, *4*, 1256–1266. https://doi.org/10.1021/cn4000428.
47. Volpe, D.A.; Tobin, G.A.M.; Mellon, R.D.; Katki, A.G.; Parker, R.J.; Colatsky, T.; Kropp, T.J.; Verbois, S.L. Uniform assessment and ranking of opioid Mu receptor binding constants for selected opioid drugs. *Regul. Toxicol. Pharmacol.* **2011**, *59*, 385–390. https://doi.org/10.1016/j.yrtph.2010.12.007.
48. Kode srl. Molecular Descriptors Calculation—Dragon—Talete srl. 2017. Available online: https://www.talete.mi.it/products/dragon_description.htm (accessed on 26 April 2026).
49. Haupt, R.L.; Haupt, S.E. Introduction to Optimization. In *Practical Genetic Algorithms*; John Wiley & Sons, Ltd.: Hoboken, NJ, USA, 2003; pp. 1–25. https://doi.org/10.1002/0471671746.ch1.
50. OECD. *(Q)SAR Assessment Framework: Guidance for the Regulatory Assessment of (Quantitative) Structure Activity Relationship Models and Predictions*; OECD Series on Testing and Assessment; OECD: Paris, France, 2023. https://doi.org/10.1787/d96118f6-en.
51. Gramatica, P.; Cassani, S.; Roy, P.P.; Kovarich, S.; Yap, C.W.; Papa, E. QSAR Modeling is not "Push a Button and Find a Correlation": A Case Study of Toxicity of (Benzo-)triazoles on Algae. *Mol. Inform.* **2012**, *31*, 817–835. https://doi.org/10.1002/minf.201200075.
52. Gramatica, P.; Sangion, A. A Historical Excursus on the Statistical Validation Parameters for QSAR Models: A Clarification Concerning Metrics and Terminology. *J. Chem. Inf. Model.* **2016**, *56*, 1127–1131. https://doi.org/10.1021/acs.jcim.6b00088.
53. Hunskaar, S.; Berge, O.-G.; Hole, K. A modified hot-plate test sensitivie to mild analgesics. *Behav. Brain Res.* **1986**, *21*, 101–108.

54. American Veterinary Medical Association. *AVMA Guidelines for the Euthanasia of Animals*; American Veterinary Medical Association: Schaumburg, IL, USA, 2020.
55. Zimmermann, M. Ethical Guidelines for Investigations of Experimental Pain in Conscious Animals. *PAIN* **1983**, *16*, 109. https://doi.org/10.1016/0304-3959(83)90201-4.

Disclaimer/Publisher's Note: The statements, opinions and data contained in all publications are solely those of the individual author(s) and contributor(s) and not of MDPI and/or the editor(s). MDPI and/or the editor(s) disclaim responsibility for any injury to people or property resulting from any ideas, methods, instructions or products referred to in the content.